



Analysis of a chaotic and a non-chaotic 3D dynamical system: the Quasi-Geostrophic omega equation and the Lorenz-96 model

Nikolaos Gkrekas*

Department of Mathematics, University of Thessaly, Lamia, 35100 Fthiotis, Greece.
Department of Mathematics, University of Kansas, Lawrence, KS 66045, USA.

Abstract

This paper delves into analyzing two 3D dynamical systems of ordinary differential equations (ODEs), namely the Quasi-Geostrophic Omega Equation and the Lorenz-96 Model. The primary objective of this paper is to analyze the chaotic and non-chaotic behavior exhibited by the QG Omega Equation and the Lorenz-96 Model in three dimensions. Through numerical simulations and analytical techniques, the author aims to characterize the existence and properties of attractors within these systems and explore their implications for atmospheric dynamics. Furthermore, we investigate how changes in initial conditions and system parameters influence the behavior of the dynamical systems. Employing a combination of numerical simulations and analytical methods, including stability analysis and Lyapunov functions, the author uncovers patterns and correlations that shed light on the mechanisms driving atmospheric phenomena. This analysis contributes to the understanding of atmospheric dynamics and has implications for weather forecasting and climate modeling, offering insights into the predictability and stability of atmospheric systems. Finally, the author presents the phase portrait of the chaotic system and visualizations of the attractors of both systems.

Keywords. Chaos, Dynamical systems, ODEs, Lorenz model, Attractors.

1991 Mathematics Subject Classification. 34H10, 37N10, 37D45.

1. INTRODUCTION

In this research, we concentrate on the topics of chaos theory and dynamical systems, with applications in meteorology. Dynamical systems theory examines how points in a given space evolve according to specific rules, often described by differential equations (Horton & Hakim [14]).

Chaos refers to the behavior of a nonlinear dynamical system that is highly sensitive to small changes in initial conditions. Due to this sensitivity, even minimal variations in starting values can lead to significantly different outcomes. A well-known example is the butterfly effect, which illustrates how a minor disturbance in one part of a deterministic nonlinear system can result in large deviations elsewhere. The butterfly effect suggests that the flap of a butterfly's wing in one side of the world might ultimately trigger a hurricane in another side (Weber [37]). Another hallmark of chaotic systems is their lack of periodic behavior. The symmetry properties of these nonlinear systems can play a crucial role in generating chaotic dynamics. recent research has increasingly focused on the symmetric features of chaotic systems (Ramadevi & Bingi [30]).

The intersection of chaos theory and meteorology dates back to the pioneering work of Edward Lorenz in the 1960s. While modeling atmospheric convection, Lorenz discovered that small changes in initial conditions in his simplified weather model could produce drastically different outcomes, a phenomenon he termed "deterministic chaos" (Lorenz [20]). This discovery challenged the prevailing belief that sufficiently detailed data would make long-term weather prediction reliably precise.

Received: 20 April 2024 ; Accepted: 20 July 2024.

* Corresponding author. Email: ngkrekas@uth.gr, gkrekas@ku.edu.

Vertical velocities are critical in ocean circulation, ocean–atmosphere interaction, and hence climate. The distribution and productivity of both autotrophic and heterotrophic plankton, key biological components, are strongly influenced by vertical advection. Consequently, there is significant interest in linking biological patchiness to physical oceanographic processes (Allen et al. [2]). Under the assumption of quasi-geostrophic (QG) balance, vertical motion can be diagnosed using a Poisson-type equation driven by the divergence of a function dependent solely on the geostrophic velocity field (Hoskins et al. [15]). This equation, known as the omega equation, can be derived from the QG vorticity equation (Billingsley [6]).

The parameterization of unresolved subgrid processes plays a substantial role in the uncertainty of weather and climate models. Both chaotic behavior and fractal structures have been observed in meteorological phenomena. Traditional deterministic parameterization approaches estimate the average or most probable subgrid-scale forcing for a given resolved-scale state. While improving these parameterizations can reduce model error to a degree, it cannot eliminate it entirely. Irreducible uncertainty stems from a lack of a clear scale separation between resolved and unresolved processes. The inherently chaotic nature of the atmosphere, which amplifies the effects of imprecise initial conditions, also contributes to the uncertainty in weather forecasts (Karimi & Paul [17]).

The Lorenz-96 system was developed as a “toy model” of the extratropical atmosphere. It offers a simplified framework to study advective nonlinearities and multiscale interactions (Lorenz & Haman [21]). The model consists of two sets of variables distributed around a latitude circle, representing different spatial scales.

Due to its chaotic nature, even small variations in initial atmospheric conditions can lead to vastly different weather patterns, exemplifying the principles of chaos theory (Lorenz & Haman [21]).

This sensitivity makes precise long-term weather forecasting inherently challenging. However, through the use of sophisticated computer models and extensive data collection, meteorologists can simulate dynamical systems with greater accuracy, thereby improving weather predictions and deepening our understanding of atmospheric behavior in the presence of chaos (Mihailović et al. [26]).

Numerical simulations facilitate the visualization of the system trajectories in phase space and help identify the presence of attractors, key structures that govern long-term behavior, (Maayah et al. [23], Maayah & Arqub [22]).

The objective of this study is to advance our understanding of atmospheric dynamics by conducting a comprehensive analysis of two fundamental dynamical systems: the Quasi-Geostrophic (QG) Omega Equation and the Lorenz-96 Model in three dimensions. Specifically, we investigate the behavior of the non-chaotic QG Omega Equation and the chaotic Lorenz-96 model. Analytical methods, including the use of a Lyapunov function, are employed to explicitly verify the existence of a global attractor in the 1D Lorenz-96 model.

We further extend the Lorenz-96 model into three dimensions, representing the full system through linear algebraic formulations involving vectors and matrices. To incorporate stochastic characteristics, two parameters in the model are modified, introducing Wiener processes and diffusion coefficients to capture statistical variability. The 3D transformation of the Lorenz-96 model is then reduced to a 2D version, followed by a simplified 2D system of ordinary differential equations (ODEs). At each stage, we utilize MATLAB to visualize attractors, vector fields, and the resulting phase portraits.

This study aims to deepen our understanding of chaotic dynamics and attractor structures within these systems—insights that hold significant implications for weather forecasting and climate modeling. By analyzing the existence and properties of attractors, we seek to improve our grasp of the fundamental processes that govern atmospheric behavior, ultimately contributing to the advancement of predictive modeling techniques in meteorology.

2. WEATHER EVENTS IN SYSTEMS OF ODES

Ordinary Differential Equations (ODEs) play a pivotal role in meteorology, providing a mathematical framework to describe and analyze the dynamical behavior of atmospheric processes, Selvam [34]. These equations capture the interactions between various atmospheric variables such as temperature, pressure, wind speed, and humidity, allowing meteorologists to model and predict weather phenomena on different spatial and temporal scales. In meteorological applications, ODEs are often employed to model atmospheric dynamics, radiation transfer, cloud formation, and other essential processes governing weather systems. Furthermore, dynamical systems theory offers powerful analytical tools to investigate the behavior of these models, allowing researchers to explore fundamental concepts such as chaos,



stability, and attractors. By applying dynamical systems analysis to meteorological ODE models, scientists gain deeper insights into the mechanisms driving weather patterns, ultimately improving forecasting capabilities and advancing the understanding of climate dynamics. In addition, climate change models, essential for assessing long-term environmental trends—are often grounded in the principles of mathematical modeling (Rizos & Gkrekas [31]).

Overall, the integration of ODEs and dynamical systems theory forms a cornerstone of modern meteorology, facilitating the study and prediction of atmospheric phenomena crucial for society’s well-being and environmental sustainability.

In this paper, we employ ODEs to describe the vertical motion of air parcels using the QG Omega equation, as well as to model the chaotic behavior of the Lorenz-96 system. These equations capture essential features of atmospheric dynamics, particularly on a latitude circle, and are widely used in meteorology and climate science to investigate large-scale weather patterns.

3. CHAOS AND FRACTALS IN METEOROLOGY

Chaos theory and fractal geometry have emerged as powerful frameworks for understanding the complexity and unpredictability of atmospheric phenomena in meteorology [17]. Chaos theory emphasizes the sensitivity of meteorological systems to initial conditions, where small differences in initial states can lead to significantly divergent outcomes over time, Annan & Hargreaves [4]. This sensitivity to initial conditions often manifests as seemingly random and erratic behavior, commonly referred to as chaos, in processes such as turbulence, convection, and evolving weather patterns (Lea et al. [19]). Fractal geometry complements chaos theory by revealing the self-similar and irregular structures that characterize atmospheric phenomena across a wide range of spatial and temporal scales. Examples include the intricate patterns of cloud formations, coastlines, and turbulent flows, which exhibit similar geometric features when observed at different levels of magnification (Millán et al. [27]). By integrating chaos theory with fractal geometry, meteorologists can gain deeper insights into the mechanisms driving atmospheric dynamics and variability (Duane [10]). Together, these frameworks provide valuable tools for analyzing and modeling complex meteorological systems, thereby enhancing weather forecasting, improving our understanding of climate variability, and supporting efforts to address challenges associated with climate change and extreme weather events.

4. NON-CHAOTIC DYNAMICAL SYSTEM: QUASI-GEOSTROPHIC OMEGA EQUATION

The Quasi-Geostrophic Omega Equation is a commonly used equation in meteorology to describe the vertical motion of air parcels in the atmosphere. It is derived from the quasi-geostrophic approximation, which is valid for large-scale, slowly varying flows in the atmosphere (Wu [39]). It first appeared as a general version, which we are not going to concentrate on, but rather as a simplified 3D variation of it. For completeness, it is expressed as below.

$$\left(\frac{\partial^2}{\partial x^2} + \frac{\partial^2}{\partial y^2}\right)\omega + f_0^2 \frac{\partial^2 \omega}{\partial p^2} = f_0 \left(\frac{\partial}{\partial x} \left(\frac{Q_y}{\sigma}\right) - \frac{\partial}{\partial y} \left(\frac{Q_x}{\sigma}\right)\right), \tag{4.1}$$

and in the form:

$$\nabla_p^2 \omega + f_0^2 \frac{\partial^2 \omega}{\partial p^2} = -f_0 \nabla_p \cdot \left(\frac{\vec{Q}}{\sigma}\right), \tag{4.2}$$

where ω is the vertical velocity in pressure coordinates (Pa/s), f_0 is the Coriolis parameter at a reference latitude, σ is the static stability parameter, Q_x and Q_y are components of the Q-vector.

The Q-vector components are given by:

$$Q_x = -\frac{R}{p} \left(\frac{\partial T}{\partial x} \cdot \frac{\partial u_g}{\partial x} + \frac{\partial T}{\partial y} \cdot \frac{\partial u_g}{\partial y}\right), \tag{4.3}$$

$$Q_y = -\frac{R}{p} \left(\frac{\partial T}{\partial x} \cdot \frac{\partial v_g}{\partial x} + \frac{\partial T}{\partial y} \cdot \frac{\partial v_g}{\partial y}\right), \tag{4.4}$$

where R is the specific gas constant for dry air, T is temperature, p is pressure, u_g and v_g are the components of the geostrophic wind in the x (east-west) and y (north-south) directions, respectively.



The Quasi-Geostrophic Omega Equation can be represented by a set of three-dimensional partial differential equations in our case, which can be simplified to a three-dimensional system of ODEs in certain scenarios (Mou et al. [28]). In most cases, we use that system to express the vertical movements, either of parcels of air, cavities, or even flow currents written as mathematical vectors (Jiao et al. [16]). One simplified form of the equation is given by:

$$\begin{cases} \frac{du}{dt} = -fv, \\ \frac{dv}{dt} = fu, \\ \frac{dw}{dt} = \frac{1}{\rho} \frac{\partial p}{\partial z}, \end{cases} \quad (4.5)$$

where u, v and w represent the zonal, meridional, and vertical components of the wind velocity, respectively, f is the Coriolis parameter, p is the pressure, and ρ is the air density.

This system describes the motion of air parcels under the influence of the Coriolis force and pressure gradients in the atmosphere (Rodrigo [33]). While it doesn't exhibit chaotic behavior, it captures the dynamics of large-scale atmospheric circulation patterns, such as those associated with the movement of high and low-pressure systems, without the complexity of chaotic behavior.

4.1. The Coriolis parameter. The Coriolis parameter f , also known as the Coriolis coefficient, is a fundamental concept in meteorology and fluid dynamics (Zhang & Yang [42]). It arises from the Earth's rotation and plays a crucial role in determining the behavior of atmospheric and oceanic motions (Yin et al. [40], Ak et al. [1]).

The Coriolis parameter f represents the effect of the Earth's rotation on moving objects or fluid parcels in a rotating reference frame, such as the atmosphere or ocean. It is defined as twice the product of the angular velocity of the Earth's rotation (Ω) and the sine of the latitude (ϕ):

$$f = 2\Omega \sin \phi, \quad (4.6)$$

where f is the Coriolis parameter, Ω is the angular velocity of the Earth's rotation (approximately 7.292×10^{-5} radians per second), and ϕ is the latitude of the location in radians.

The Coriolis parameter f introduces a fictitious force, known as the Coriolis force, which acts perpendicular to the direction of motion of an object or fluid parcel moving within the rotating reference frame. This force arises due to the relative motion between the rotating Earth and the moving object or fluid parcel. The Coriolis force deflects moving objects to the right in the Northern Hemisphere and to the left in the Southern Hemisphere, leading to the rotation of large-scale weather systems such as cyclones and anticyclones.

In meteorology, the Coriolis parameter f is a key factor influencing atmospheric dynamics, including the formation of winds, the development of weather systems, and the global circulation patterns. It contributes to phenomena such as the generation of trade winds, the formation of cyclones and anticyclones, and the behavior of atmospheric waves Koriko et al. [18].

For completeness, we rewrite the system (4.5) with the Coriolis parameter (4.6) and we obtain:

$$\begin{cases} \frac{du}{dt} = -2\Omega v \sin \phi, \\ \frac{dv}{dt} = 2\Omega u \sin \phi, \\ \frac{dw}{dt} = \frac{1}{\rho} \frac{\partial p}{\partial z}. \end{cases} \quad (4.7)$$

4.2. Visualization and plots about the QG Omega Equation. We elaborate on different aspects of the non-chaotic attractor of the QG Omega equation and the vector field in two and three dimensions using MATLAB software. These outputs are more thoroughly explained in Figures 1 and 2. In the first output, the vector velocity field for the QG Omega Equation in two-dimensions and its generalization three-dimensional space are shown. In the second output, the 3D attractor for QG Omega Equation is shown. The attractor in non-chaotic, and the system exhibits complete stability in all its orbits.



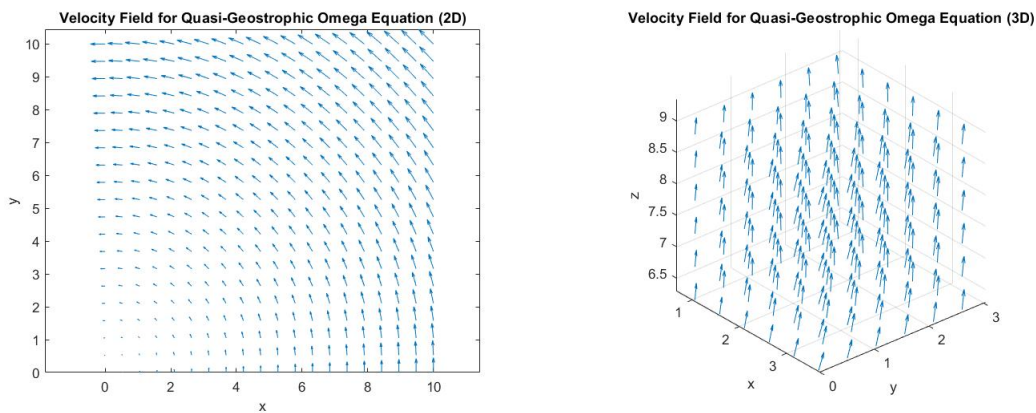


FIGURE 1. The vector space of the QG Omega equation in 2D plane and 3D space, where the Coriolis parameter $f = 1$, and gravitational constant $g = 9.81$. (Source: Author’s own elaboration (see 7)).

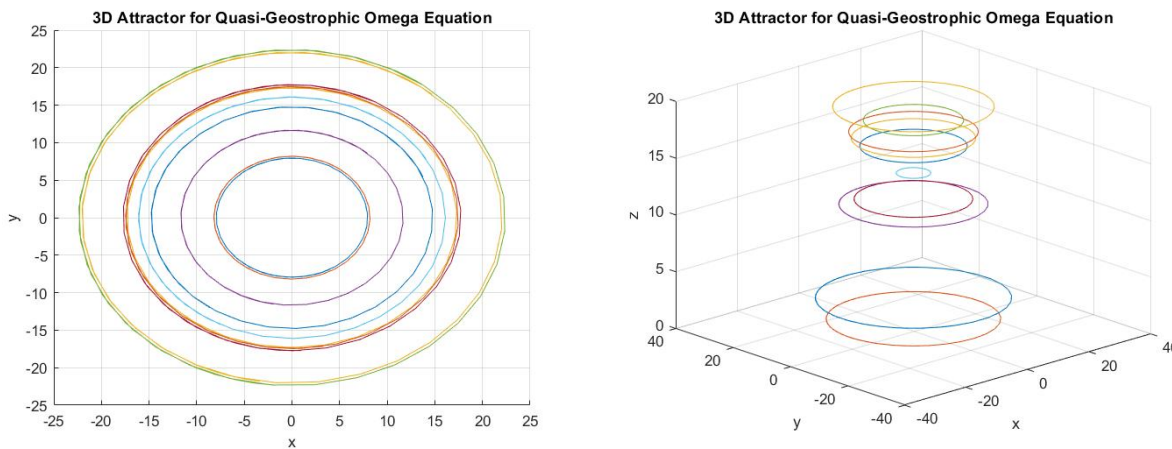


FIGURE 2. The non-chaotic attractor for the QG Omega Equation Dynamical system with stable points from the 2D and 3D perspective, where the Coriolis parameter $f = 1$, number of trajectories=10 and initial conditions= 20*random triplets of the trajectories. (Source: Author’s own elaboration (see 7)).

5. CHAOTIC DYNAMICAL SYSTEM: LORENZ ATTRACTOR

The Lorenz system of equations is a simplified model originally developed to study atmospheric convection. Although it may not capture specific meteorological events, it exhibits chaotic behavior that shares some qualitative features with atmospheric phenomena. Some examples of applications of the Lorenz model are briefly stated below.

- (1) **Turbulence and Convective Instability:** The Lorenz system can exhibit chaotic behavior, characterized by rapid and unpredictable changes in state variables. This behavior resembles the turbulent and convective processes observed in the atmosphere, especially in regions prone to thunderstorms and convective activity. The convective instabilities drive the lateral structure of the flow, eventually resulting in finer-scale vortical motion with components in the $x-z$ direction that enhance energy dissipation and mixing, characteristic of a turbulent flow.



- (2) **Rosby Waves and Atmospheric Circulation Patterns:** The Lorenz system's attractor can display intricate patterns reminiscent of atmospheric circulation patterns, such as Rossby waves. These large-scale planetary waves play a crucial role in shaping weather patterns, including the development of high and low-pressure systems, jet streams, and storm tracks.
- (3) **Teleconnections and Climate Variability:** Chaotic systems like the Lorenz model are sensitive to initial conditions, leading to the emergence of complex structures on their attractors. Analogously, atmospheric teleconnections, such as the El Niño-Southern Oscillation (ENSO), arise from the nonlinear interactions between ocean and atmospheric processes, resulting in widespread climate variability across different regions of the globe.
- (4) **Irregular Weather Patterns:** The Lorenz system's chaotic behavior can also resemble irregular weather patterns observed in the real atmosphere. For instance, the unpredictable nature of chaotic trajectories may capture the sporadic occurrence of extreme weather events, such as heatwaves, cold spells, or sudden shifts in atmospheric circulation.
- (5) **Climate Regime Shifts:** Changes in the behavior of the Lorenz system, such as bifurcations and transitions between different attractor states, can be analogous to abrupt climate regime shifts observed in Earth's climate system. These shifts, often associated with changes in external forcing or feedback mechanisms, can lead to significant alterations in regional and global climate patterns over time.

While the Lorenz system provides a simplified representation of atmospheric dynamics, it offers valuable insights into the underlying mechanisms of chaos and complexity in meteorological systems (Shen et al. [35]). However, direct comparisons between the Lorenz model and specific meteorological events should be made with caution, as the model's dynamics may not fully capture the complexities of real-world atmospheric processes. The evolution rule of a dynamical system is a function that describes what future states follow from the current state. Often, the function is deterministic, that is, for a given time interval, only one future state follows from the current state. In our case, we do not use such a function because we investigate the systems as a general version and a methodology for studying these types of 3D chaotic dynamical systems.

5.1. General Lorenz three-dimensional model.

$$\begin{cases} \frac{dx}{dt} = \sigma(y - x), \\ \frac{dy}{dt} = x(\rho - z) - y, \\ \frac{dz}{dt} = xy - \beta z. \end{cases} \quad (5.1)$$

The attractors' existence and characteristics are determined by the system's starting circumstances and the parameters σ , ρ , and β .

These parameters were introduced by Edward Lorenz in his seminal paper "Deterministic Nonperiodic Flow" (Lorenz [20]) to study atmospheric convection and represent certain physical aspects of the system. Here, σ is the one that controls the rate of change of the system's state variable x . It represents the Prandtl number, which characterizes the ratio of momentum diffusivity to thermal diffusivity in fluid dynamics. In the context of the Lorenz system, σ influences the speed at which the system variables evolve in time. Higher values of σ result in faster evolution of the system.

ρ is the parameter that represents the Rayleigh number, which characterizes the ratio of buoyancy forces to viscous forces in fluid dynamics. In the Lorenz system, ρ determines the intensity of the convective motion and the overall scale of the system's behavior. Higher values of ρ lead to more vigorous convection and often result in the emergence of chaotic behavior in the system.

Finally, β is the parameter that represents the aspect ratio relating the dimensions of the system. In the context of the Lorenz system, β controls the spatial scale over which the system's variables interact. It is related to the geometry of the convective cells and the feedback mechanisms between different components of the system. Changes in β can lead to transitions in the system's behavior, such as bifurcations and the emergence of multiple attractors.

The Lorenz system is known to behave chaotically under specific parameter regimes. In particular, there is a set of parameter values for which the system displays sensitive dependence on initial circumstances, non-periodic trajectories,



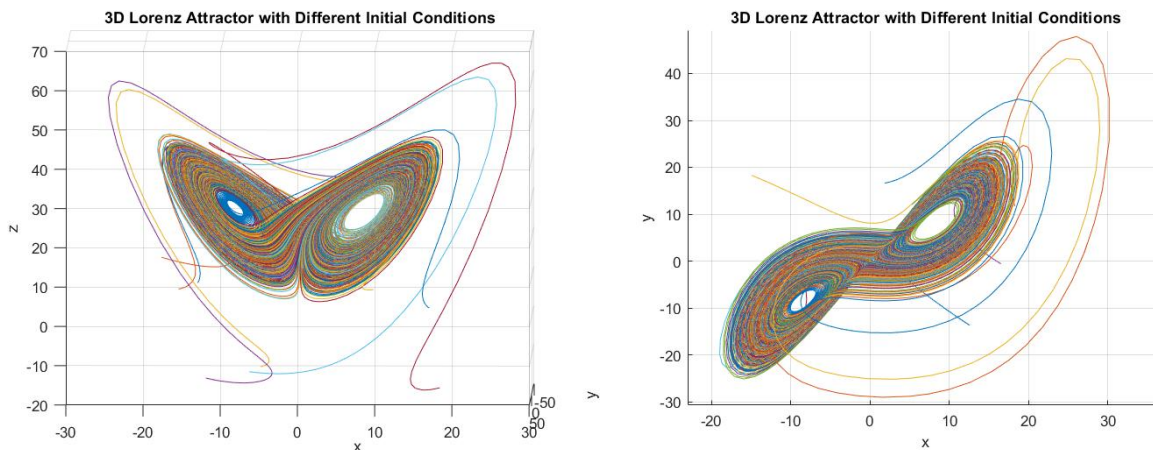


FIGURE 3. Two representations of the 3D Lorenz attractor on two dimension projections, the $x - z$ plane and $x - y$ plane. The initial conditions were selected randomly in a closed interval $[1 - 10]$. (Source: Author's own elaboration (see 7)).

and an unusual attractor in phase space. This strange attractor is a geometrically complicated set that attracts system trajectories and describes the system's chaotic behavior.

However, it is crucial to highlight that the existence and features of attractors in the Lorenz system change depending on the parameter values.

In the next section, visualization is utilized because researchers believe that the visualization of a model is a very effective way of understanding the behavior (Rizos & Gkrekas [32]).

5.2. Common Visualization of the simple 3D Lorenz attractor. We elaborate using MATLAB software on different aspects of a Lorenz strange attractor with varying initial conditions within a given closed interval. The outputs are thoroughly explained in Figures 3, 4, and 5.

5.3. The Lorenz-96 model. The Lorenz-96 model, a variant derived from the iconic Lorenz system, stands as a cornerstone in the study of complex dynamical systems within meteorology. Originating from Edward Lorenz's pioneering work on atmospheric convection, the Lorenz-96 model extends the original three-variable Lorenz equations to a higher-dimensional framework, capturing more intricacies of atmospheric dynamics (Amemiya et al. [3]). Unlike its predecessor, which primarily explores the behavior of a single convective cell, the Lorenz-96 model represents a coupled system of nonlinear ordinary differential equations, mimicking the interactions between grid points in a simplified atmospheric circulation model. Widely recognized for its ability to reproduce fundamental features of atmospheric phenomena, such as wave propagation, phase transitions, and spatiotemporal chaos, the Lorenz-96 model serves as a valuable tool in meteorology for understanding and predicting a broad spectrum of weather-related processes. The model describes a single scalar quantity as it evolves on a circular array of sites, undergoing forcing, dissipation, and rotation-invariant advection. Its applications span from elucidating the mechanisms underlying climate variability and teleconnections to exploring the predictability of weather patterns and assessing the impacts of external forcings on atmospheric dynamics. Through its representation of complex, nonlinear interactions among atmospheric variables, the Lorenz-96 model continues to offer valuable insights into the emergent behaviors of meteorological systems, contributing significantly to the advancement of atmospheric science and forecasting capabilities. Initially, Lorenz intended to create this system as a test problem for numerical weather prediction.

5.3.1. Deriving the one-dimensional Lorenz-96 model. The Lorenz-96 model is derived from the original Lorenz equations mentioned above in (5.1) by considering a discretization of space. In the original Lorenz equations, the variables x , y , and z represent the state variables of the system, which describe the evolution of fluid flow in continuous space. In

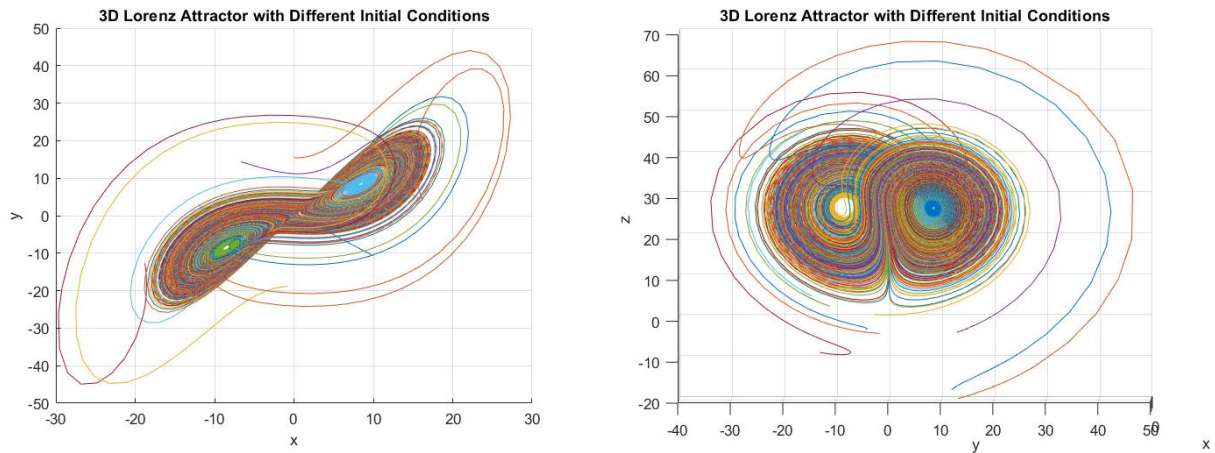


FIGURE 4. Two representations of the 3D Lorenz attractor on two dimension projections, the $x - y$ plane and $y - z$ plane. The initial conditions were selected randomly in a closed interval $[1 - 10]$. (Source: Author's own elaboration (see 7)).

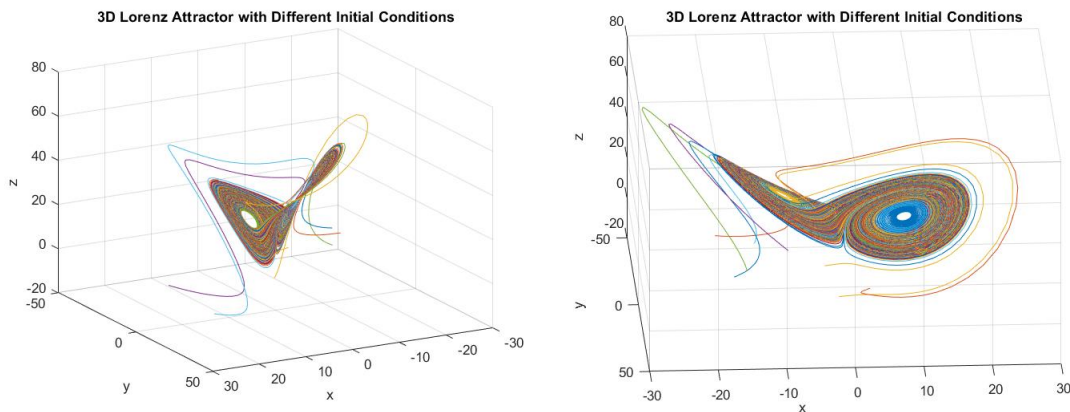


FIGURE 5. Two representations of another Lorenz chaotic attractor with random initial conditions through an closed interval $[1, 10]$ in three dimensions (Source: Author's own elaboration (see 7)).

the Lorenz-96 model, we discretize the space into a set of N grid points or “cells” denoted by x_1, x_2, \dots, x_N , where each grid point represents a location in space. The dynamics of each grid point in the Lorenz-96 model are influenced by its neighboring grid points, meaning that each grid point x_i interacts with itself and its nearest neighbours x_{i-1}, x_{i+1} .

The evolution of each grid point x_i over time is governed by a set of ordinary differential equations (ODEs), which describe the rate of change of each grid point's state variable with respect to time. In the Lorenz-96 model, the coupling between grid points is introduced through a nonlinear term that represents the influence of neighboring grid points on another. This coupling term captures the interaction between adjacent grid points and is essential for generating complex dynamical behavior. The Lorenz-96 model introduces parameters such as the strength of coupling between grid points and the rate of dissipation of energy. These parameters control the behavior of the system and can be adjusted to study different phenomena. The Lorenz-96 equations take the form of a set of coupled ordinary differential equations, where each equation represents the time evolution of a single grid point. The equations describe

how the state variables at each grid point change over time, influenced by both the local dynamics and the interactions with neighboring grid points. By discretizing space and considering the interactions between adjacent grid points, the Lorenz-96 model captures the essential features of atmospheric dynamics in a simplified and computationally tractable framework. The grid points or the complete lattice can aid us in expressing and observing the behavior of the system. For all considered atmospheric variables and constants, the discretized space helps simplify the problem, yielding more consistent results.

The Lorenz-96 equations describe the evolution of a set of N variables x_i , each representing the state of a grid point in a discretized spatial domain:

$$\frac{dx_i}{dt} = (x_{i+1} - x_{i-2})x_{i-1} - x_i + F - D \sum_{j=1}^N x_j, \tag{5.2}$$

where N is the number of grid points, F is a forcing term representing external influences or sources of energy, D is a damping coefficient controlling the rate of dissipation of energy.

These equations represent the time rate of change of each grid point x_i , which is influenced by its neighboring grid points as well as external forcing and dissipation effects. The term $(x_{i+1} - x_{i-2})x_{i-1}$ captures the nonlinear interaction between adjacent grid points, while the summation term $\sum_{j=1}^N x_j$ represents the coupling between all grid points in the system.

5.3.2. A variation of the Lorenz-96 model describing the time evolution of each grid point x_i in a discretized spatial domain. The general Lorenz system (5.1) can be thought of as a simplified representation of atmospheric convection, with x, y and z representing different atmospheric variables (e.g., temperature, pressure, and wind speed). In the Lorenz-96 model, we extend this concept to a one-dimensional grid, where each variable x_i represents the state of the atmosphere at a different grid point i . To derive this variant of the Lorenz-96 model, similarly to the general one, we discretize the spatial dimension, introducing a set of N grid points along a latitude circle, and we introduce periodic boundary conditions to represent the circular nature of the domain. This form of the Lorenz-96 equation captures the essential features of atmospheric dynamics on a latitude circle and is commonly used in meteorology and climate science to study large-scale weather patterns. Therefore, after these modifications, we obtain the following equation.

$$\frac{dx_i}{dt} = (x_{i+1} - x_{i-2})x_{i-1} - x_i + F - \frac{c}{K}(x_i - \bar{x}), \tag{5.3}$$

where x_i represents the state variable at grid point i , t represents time, F represents a forcing term applied uniformly across all grid points, c represents a parameter controlling the strength of coupling between grid points, K is the total number of grid points, and \bar{x} represents the mean value of x over all grid points, given by the equation $\bar{x} = \frac{1}{N} \sum_{i=1}^N x_i$.

5.3.3. Proof of existence of an attractor for the Lorenz-96 model. In this version, the model has changed a bit. Specifically, the term $(x_i - \bar{x})$, the difference of each term with the mean value of x_i has been replaced by the summation $\sum_{j=1}^N x_j$ representing the coupling between all grid points in the system.

$$\frac{dx_i}{dt} = (x_{i+1} - x_{i-2})x_{i-1} - x_i + F - \frac{c}{K} \sum_{j=1}^N x_j. \tag{5.4}$$

Proposition 5.1. *Trajectories of the Lorenz-96 model are bounded in the state space.*

Proof. We define the trajectory of the system as $x(t)$, and we define the Lyapunov function as below.

$$V(x) = \frac{1}{2} \sum_{i=1}^N (x_i - \bar{x})^2. \tag{5.5}$$

Then we compute the derivative of the Lyapunov function:

$$\frac{dV}{dt} = \sum_{i=1}^N (x_i - \bar{x}) \frac{dx_i}{dt} = \sum_{i=1}^N (x_i - \bar{x}) [(x_{i+1} - x_{i-2})x_{i-1} - x_i + F - \frac{c}{K} \sum_{j=1}^N x_j]. \tag{5.6}$$



We know that F is bounded as a constant, each term $(x_i - \bar{x})$ is bounded because both x_i and \bar{x} are finite, and $\sum_{j=1}^N x_j$ is bounded due to the boundedness of x_i . Therefore, $\frac{dV}{dt}$ is bounded, and hence the trajectories are bounded in the state space. \square

Proposition 5.2. *There exists a compact invariant set A to which trajectories converge as time approaches infinity.*

Proof. Let Ω be the set of all possible states x such that each variable x_i is bounded within a certain interval $[a, b]$ for all $i = 1, 2, \dots, N$. We define Ω as:

$$\Omega = \{x \in \mathbb{R}^N : a \leq x_i \leq b, \forall i = 1, 2, \dots, N\}, \quad (5.7)$$

where a and b are constants representing the lower and upper bounds of the variables x_i , respectively.

We must demonstrate that trajectories starting in Ω remain in Ω for all time. This can be shown by analyzing the dynamics of the Lorenz-96 equations and showing that if $x(0) \in \Omega$, then $x(t) \in \Omega$ for all $t \geq 0$.

Since the dynamics of the Lorenz-96 model are continuous and smooth, and since x_i is initially bounded, the trajectories will remain within the interval $[a, b]$ for all time.

To establish that Ω is compact, we need to show that it is closed and bounded. The closedness follows directly from the definition of Ω . To show boundedness, we can use the fact that each variable x_i is bounded within the interval $[a, b]$, implying that Ω is bounded.

By showing that trajectories starting from Ω remain within Ω for all time and that Ω is a compact subset of the state space, we conclude that Ω is an invariant set for the Lorenz-96 model. Since Ω is compact and invariant, it serves as the desired invariant set A to which trajectories converge. \square

Proposition 5.3. *Nearby trajectories converge to the invariant set A as time approaches infinity.*

Proof. We define a metric $d(x, y)$ on the state space \mathbb{R}^N to measure the distance between two trajectories $x(t), y(t)$. We choose the common Euclidean metric with the formula:

$$d(x, y) = \|x - y\| = \sqrt{\sum_{i=1}^N (x_i - y_i)^2}. \quad (5.8)$$

Next, we choose initial conditions for two trajectories $x(t)$ and $y(t)$ that are sufficiently close, i.e.,

$$d(x(0), y(0)) < \epsilon, \quad (5.9)$$

where ϵ is an arbitrarily small positive value representing their initial separation. We want to show that the distance between trajectories $x(t)$ and $y(t)$ decays over time. This can be expressed as:

$$d(x(t), y(t)) \leq K \exp^{-\lambda t} d(x(0), y(0)), \quad (5.10)$$

where $d(x(0), y(0))$ is the distance between the initial conditions of the trajectories, K , not related to the previous K in (5.4), and λ are constants, and t is time.

We can use the Lyapunov function $V(x)$ from (5.5) to derive an inequality involving the time derivative of the Lyapunov function, as done in (5.6) that can be used to bound the distance between trajectories. We expand the Equation (5.6).

$$\frac{dV}{dt} = \sum_{i=1}^N (x_i - \bar{x}) [(x_{i+1} - x_i)x_{i-1} - (x_i - x_{i-2})x_{i-1} - x_i + F - \frac{c}{K} \sum_{j=1}^N x_j], \quad (5.11)$$

$$\frac{dV}{dt} = \sum_{i=1}^N (x_i - \bar{x}) [(x_{i+1} - x_i)x_{i-1} - (x_i - x_{i-2})x_{i-1} - x_i] + F \sum_{i=1}^N (x_i - \bar{x}) - \frac{c}{K} \sum_{i=1}^N (x_i - \bar{x}) \sum_{j=1}^N x_j. \quad (5.12)$$

Grouping the terms, we obtain:

$$\frac{dV}{dt} = \sum_{i=1}^N (x_i - \bar{x}) [(x_{i+1} - x_i)x_{i-1} - (x_i - x_{i-2})x_{i-1} - x_i] + F \sum_{i=1}^N (x_i - \bar{x}) - \frac{c}{K} \left(\sum_{i=1}^N x_i \right)^2. \quad (5.13)$$



Then, to bound the distance between trajectories, $\frac{dV}{dt}$ can be rewritten as

$$\frac{dV}{dt} = - \sum_{i=1}^N [(x_i - \bar{x})^2 - (x_{i+1} - x_i)(x_i - x_{i-2})x_{i-1}] - \frac{c}{K} \left(\sum_{i=1}^N x_i \right)^2 + F \sum_{i=1}^N (x_i - \bar{x}), \tag{5.14}$$

where the terms involving $(x_i - \bar{x})$ are bounded due to the boundedness of trajectories, and the sum of squares term is also bounded. Therefore $\frac{dV}{dt}$ is bounded.

By showing that the distance between trajectories decays exponentially, we can conclude that nearby trajectories converge to a compact invariant set A as $t \rightarrow \infty$. □

Remark 5.4. The invariant set A is attracting and minimal.

Next, some definitions will be given without proof, just for completeness.

Definition 5.5. Attracting property is when an invariant set A is attracting if trajectories starting from nearby initial conditions tend to converge to A as time evolves.

Definition 5.6. Minimal property is when an invariant set A is minimal if there exists no proper subset of A that is also invariant and attracting.

By analyzing the properties of the invariant set A , including its attracting and minimal properties, stability characteristics, geometric structure, and numerical verification, we can determine whether it satisfies the criteria of an attractor for the Lorenz-96 model.

5.3.4. *The transformation of the Lorenz-96 model in three dimensions.* In this section, the one-dimensional Lorenz-96 model in Equation (5.4) is transformed into a three-dimensional model in the real space \mathbb{R}^3 . The novelty of this paper is this transformation, its visualization, and further study on the existing attractor and behavior of the following system:

$$\begin{cases} \frac{dx_i}{dt} = (x_{i+1} - x_{i-2})x_{i-1} - x_i + F - \frac{c}{K}(x_i - \bar{x}), \\ \frac{dy_i}{dt} = (y_{i+1} - y_{i-2})y_{i-1} - y_i + F - \frac{c}{K}(y_i - \bar{y}), \\ \frac{dz_i}{dt} = (z_{i+1} - z_{i-2})z_{i-1} - z_i + F - \frac{c}{K}(z_i - \bar{z}). \end{cases} \tag{5.15}$$

Similarly with the one-dimensional model, x_i, y_i, z_i represent the state variables at grid point i for different orientations, t represents time, F represents a forcing term applied uniformly across all grid points, c represents a parameter controlling the strength of coupling between grid points, K is the total number of grid points and $\bar{x}, \bar{y}, \bar{z}$ represent the mean values of x, y and z respectively, over all grid points.

This is the traditional way of expressing this chaotic dynamical system that will be utilized in the next section of the visualization. We are also going to transform the system into a matrix form, in order to make the system more easily handled; this method is used in systems of ODEs, such as epidemiology with systems of fractional derivatives (see Gkrekas [12], Maayah et al. [24]).

First, define the matrix F as the set of derivatives of each value of the vector x as mentioned below

$$\frac{d\mathbf{x}}{dt} = \mathbf{F}(\mathbf{x}). \tag{5.16}$$



The vector and the matrix of the derivatives are

$$\mathbf{x} = [x_1, x_2, \dots, x_n, y_1, y_2, \dots, y_n, z_1, z_2, \dots, z_n]^T, \quad (5.17)$$

$$\mathbf{F}(\mathbf{x}) = \begin{bmatrix} (x_2 - x_{n-1})x_{n-2} - x_1 + F - \frac{c}{K}(x_1 - \bar{x}) \\ (x_3 - x_n)x_{n-1} - x_2 + F - \frac{c}{K}(x_2 - \bar{x}) \\ \vdots \\ (y_2 - y_{n-1})y_{n-2} - y_1 + F - \frac{c}{K}(y_1 - \bar{y}) \\ (y_3 - y_n)y_{n-1} - y_2 + F - \frac{c}{K}(y_2 - \bar{y}) \\ \vdots \\ (z_2 - z_{n-1})z_{n-2} - z_1 + F - \frac{c}{K}(z_1 - \bar{z}) \\ (z_3 - z_n)z_{n-1} - z_2 + F - \frac{c}{K}(z_2 - \bar{z}) \end{bmatrix}. \quad (5.18)$$

Next, define a new vector X representing the full three-dimensional state, and a vector U for inputs, so that the general system can be written as:

$$\frac{d\mathbf{X}}{dt} = \mathbf{A}\mathbf{X} + \mathbf{B}\mathbf{U}, \quad (5.19)$$

The vector X is:

$$\mathbf{X} = [x_1 \quad \dots \quad x_n \quad y_1 \quad \dots \quad y_n \quad z_1 \quad \dots \quad z_n]^T, \quad (5.20)$$

The input vector U is:

$$\mathbf{U} = \begin{bmatrix} u_1 \\ u_2 \\ \vdots \\ u_m \end{bmatrix}, \quad (5.21)$$

The general form of the matrices A and B are the following.

$$\mathbf{A} = \begin{bmatrix} A_1 & A_2 & \dots & A_n & 0 & 0 & \dots & 0 & 0 & 0 \\ 0 & A_1 & A_2 & \dots & A_n & 0 & \dots & 0 & 0 & 0 \\ 0 & 0 & A_1 & A_2 & \dots & A_n & \dots & 0 & 0 & 0 \\ \vdots & \vdots & \vdots & \vdots & \vdots & \vdots & \ddots & \vdots & \vdots & \vdots \\ 0 & 0 & 0 & 0 & \dots & 0 & A_1 & A_2 & \dots & A_n \end{bmatrix}, \quad (5.22)$$

$$\mathbf{B} = \begin{bmatrix} B_1 & B_2 & \dots & B_n & 0 & 0 & \dots & 0 & 0 & 0 \\ 0 & B_1 & B_2 & \dots & B_n & 0 & \dots & 0 & 0 & 0 \\ 0 & 0 & B_1 & B_2 & \dots & B_n & \dots & 0 & 0 & 0 \\ \vdots & \vdots & \vdots & \vdots & \vdots & \vdots & \ddots & \vdots & \vdots & \vdots \\ 0 & 0 & 0 & 0 & \dots & 0 & B_1 & B_2 & \dots & B_n \end{bmatrix}, \quad (5.23)$$

Considering the vector of $B_i = 1$ followed by zeros, this can be expressed as a “block” of ones along the diagonal since the system is diagonal. Hence, the matrix B can be represented as the identity matrix:

$$\mathbf{B} = \begin{bmatrix} 1 & 0 & \dots & 0 \\ 0 & 1 & \ddots & \vdots \\ \vdots & \ddots & \ddots & 0 \\ 0 & \dots & 0 & 1 \end{bmatrix}, \quad (5.24)$$

Similarly, the matrix A can be written using the terms $A_i = (x_{i+1} - x_{i-2})x_{i-1} - 1 - \frac{c}{K}$, assuming $F = 1$ for simplicity. The matrix looks like this:



$$\mathbf{A} = \begin{bmatrix} (x_2 - x_{n-1})x_{n-2} - 1 - \frac{c}{K} & (x_3 - x_n)x_{n-1} & \cdots & (x_n - x_{n-3})x_{n-2} \\ (x_1 - x_{n-2})x_{n-1} & (x_2 - x_{n-1})x_{n-2} - 1 - \frac{c}{K} & \ddots & \vdots \\ \vdots & \vdots & \ddots & \vdots \\ (x_{n-1} - x_{n-4})x_{n-3} & \cdots & (x_1 - x_{n-2})x_{n-1} & (x_2 - x_{n-1})x_{n-2} - 1 - \frac{c}{K} \end{bmatrix}. \tag{5.25}$$

In the stochastic form of the dynamical system previously discussed, randomness is introduced into the system dynamics to account for uncertainties or external disturbances Črnjarić-Žic et al. [9]. This is achieved by augmenting the deterministic equations with stochastic terms, typically represented by Wiener processes (Petromichelakis & Kougioumtzoglou [29], Gagne et al. [11]). The state evolution is governed by a set of differential equations that include both deterministic and stochastic components (Wilks [38]). The deterministic part captures the underlying dynamics of the system, while the stochastic part introduces random fluctuations or noise (Brajard et al. [7]). The coupling between the stochastic noise and the system dynamics is represented by a matrix G , which scales the magnitude of the noise affecting each state variable. By incorporating stochastic elements, the model provides a more comprehensive framework for representing real-world systems where uncertainties and variability play significant roles, such as fractional-order models (Badawi et al. [5]). This approach allows for a more realistic representation of system behavior and enables the analysis of system performance under uncertain conditions.

$$\begin{cases} \frac{dx_i}{dt} = (x_{i+1} - x_{i-2})x_{i-1} - x_i + F - \frac{c}{K}(x_i - \bar{x}) + \sqrt{D_x} \frac{dW_x}{dt}, \\ \frac{dy_i}{dt} = (y_{i+1} - y_{i-2})y_{i-1} - y_i + F - \frac{c}{K}(y_i - \bar{y}) + \sqrt{D_y} \frac{dW_y}{dt}, \\ \frac{dz_i}{dt} = (z_{i+1} - z_{i-2})z_{i-1} - z_i + F - \frac{c}{K}(z_i - \bar{z}) + \sqrt{D_z} \frac{dW_z}{dt}, \end{cases} \tag{5.26}$$

where D_x, D_y, D_z are diffusion coefficients and dW_x, dW_y, dW_z are Wiener processes. The equation with the matrices is transformed accordingly for the stochastic form of the Lorenz-96 model variation:

$$\frac{d\mathbf{X}}{dt} = \mathbf{A}\mathbf{X} + \mathbf{B}\mathbf{U} + \mathbf{G}\mathbf{W}, \tag{5.27}$$

where the vector W , containing the Wiener processes that introduce random coefficients into our chaotic model, is expressed as follows:

$$\mathbf{W} = [dW_{x_1} \quad \cdots \quad dW_{x_n} \quad dW_{y_1} \quad \cdots \quad dW_{y_n} \quad dW_{z_1} \quad \cdots \quad dW_{z_n}]^T, \tag{5.28}$$

and the diagonal matrix G , containing the square roots of the diffusion coefficients, is

$$\mathbf{G} = \begin{bmatrix} \sqrt{D_x} & 0 & \cdots & 0 & 0 & \cdots & 0 \\ 0 & \sqrt{D_x} & \cdots & 0 & 0 & \cdots & 0 \\ \vdots & \vdots & \ddots & \vdots & \vdots & \ddots & \vdots \\ 0 & 0 & \cdots & \sqrt{D_y} & 0 & \cdots & 0 \\ 0 & 0 & \cdots & 0 & \sqrt{D_y} & \cdots & 0 \\ \vdots & \vdots & \ddots & \vdots & \vdots & \ddots & \vdots \\ 0 & 0 & \cdots & 0 & 0 & \cdots & \sqrt{D_z} \end{bmatrix}. \tag{5.29}$$

The matrix form of the stochastic chaotic dynamical system, particularly evident in the 3D Lorenz-96 model, offers significant advantages for both computational methods and analytic approximations of solutions. By encapsulating the system’s dynamics into matrices representing deterministic, control, and stochastic components, computational methods such as numerical integration techniques become more tractable and efficient. These methods can exploit the matrix structure to efficiently propagate the system’s state forward in time, enabling the simulation of complex behaviors and the exploration of parameter spaces. Furthermore, the matrix formulation lends itself well to analytic approximations, facilitating the development of reduced-order models and analytical insights into the system’s behavior (Zhang et al. [41]). By leveraging the matrix form, researchers can apply a variety of mathematical tools, including linear algebra and spectral analysis, to gain a deeper understanding and make predictions about the system’s evolution and properties (Gkrekas [12], He & Cao [13]). Thus, the matrix representation enhances both computational and



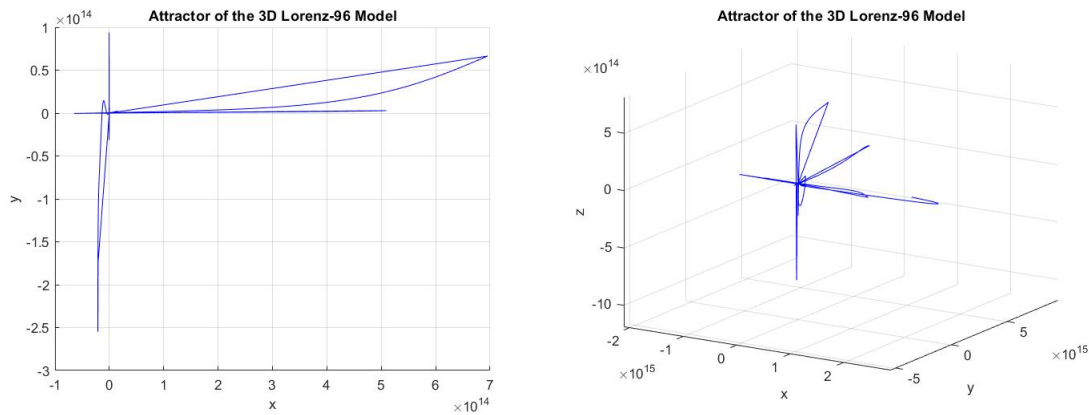


FIGURE 6. The chaotic attractor of the 3D variation of the Lorenz-96 model that we study, with random initial conditions. (Source: Author’s own elaboration (see 7)).

analytical capabilities, enabling comprehensive investigations into the dynamics and emergent phenomena of the 3D Lorenz-96 chaotic system, which is important for future research.

5.4. Visualizations of the Lorenz-96 model. The attractor we get is chaotic and when the Lorenz-96 model is projected in 3D we obtain the output in Figure 6. In this figure, there is our variation and we observe the attractor on the $x - y$ plane and the three-dimensional real space.

From the system (5.15) we transform it in 2D in order to examine the behavior of the system and draw the phase portrait and the orbits of the system. We set the variable z as a parameter where $z_i = \frac{c}{K}(z_i - \bar{z})$ in order to eliminate it. Therefore, we obtain the two dimensional system

$$\begin{cases} \frac{dx_i}{dt} = (x_{i+1} - x_{i-2})x_{i-1} - x_i + F - z_i, \\ \frac{dy_i}{dt} = (y_{i+1} - y_{i-2})y_{i-1} - y_i + F - z_i. \end{cases} \tag{5.30}$$

In this state the ODEs are recursive. In order to get the phase portrait, we have to further minimize or generalize the system, obtaining first-order ODEs. So, by simplifying further, we get

$$\begin{cases} x' = (x_{i+1} - x_{i-2})x_{i-1} - x_i + F - z_i, \\ y' = (y_{i+1} - y_{i-2})y_{i-1} - y_i + F - z_i, \end{cases} \tag{5.31}$$

$$\begin{cases} x' = (x - y)x - x + F - z, \\ y' = (y - x)y - y + F - z. \end{cases} \tag{5.32}$$

By utilizing the (5.32) we get Figure 7.

6. DISCUSSION

The exploration of the Quasi-Geostrophic Omega Equation (QG Omega Equation) and the Lorenz-96 Model in this study has revealed intriguing insights into the dynamics of atmospheric systems. The QG Omega Equation, a non-chaotic dynamical system, demonstrates stable and predictable behavior, reflecting the fundamental mechanisms underlying large-scale weather phenomena. Our analysis has unveiled the presence of attractors within this system, showcasing the convergence of trajectories towards distinct equilibrium states. These findings align with theoretical expectations and underscore the utility of the QG Omega Equation as a tool for studying the dynamics of atmospheric vertical motion.



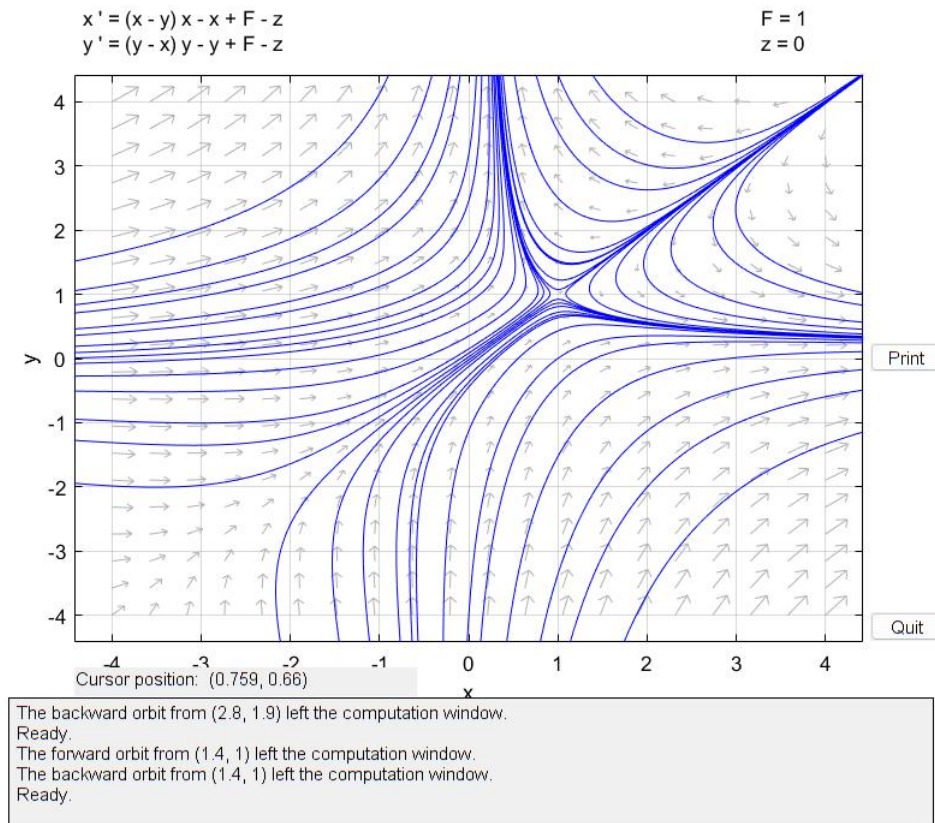


FIGURE 7. The phase portrait of the system (5.32) for parameter values $F = 1$ and with the axis $z = 0$ as fixed on the pplane8 MATLAB extension for 1st order ODEs (Source: Author’s own elaboration).

Conversely, the investigation of the Lorenz-96 Model has unraveled the intricate nature of chaotic behavior in atmospheric systems (Sun et al. [36]). Characterized by sensitive dependence on initial conditions, the Lorenz-96 Model exhibits complex dynamics that defy simple prediction (Maiocchi et al. [25]). Through numerical simulations and analytical techniques, we have elucidated the presence of strange attractors within this system, revealing the emergence of intricate patterns and structures in phase space. These findings underscore the inherent complexity of atmospheric dynamics and highlight the challenges associated with long-term weather forecasting.

Moreover, the transformation of these dynamical systems into matrix forms and the exploration of stochastic representations have provided additional insights into their underlying mechanisms, such as more efficient numerical approximations using linear algebra and dynamics of random events and probabilities (Broomhead et al. [8], Zheng & Li [43]). By abstracting the systems into mathematical frameworks, we gain a deeper understanding of the interplay between variables and the emergence of emergent behaviors. These insights not only enhance our theoretical understanding but also offer practical implications for weather forecasting and climate modeling efforts.

During the numerical approximations that we did using MATLAB, we created in the first figure the 2D plane and the 3D space where the system of the QG Omega equation is valid. By observing the rotation of the vectors in the space, we can determine the orbital behavior of the system. In the second figure, we depict the attractor of the QG Omega equation in 3D with stable closed circular orbits. This attractor is not chaotic and the behavior of the stable orbit is parallel to each other on the vertical axis, but with the same center, due to the stability of solutions. In the third and fourth figures, we observe the behavior of the chaotic Lorenz attractor and its projections on the 2D plane



for random initial conditions in a fixed closed interval, leading to the chaotic complex images that orbits change the whole trajectory with a small change in initial or boundary conditions. The fifth figure is the 3D shape of a Lorenz attractor with the same initial conditions as in the previous figures. In the sixth figure, we see the graph of the chaotic attractor of the variation of the Lorenz-96 model in 3d space and its projection on the real plane, where the outer bound of the attractor can be calculated and the behavior can be observed more thoroughly. Finally, in the seventh and last figure, we see the phase portrait that depicts the behavior of the 2D minimized variation of the 3D Lorenz-96 transformed model showing the stability of the system solutions and the orbits, where we can observe the changes in stable and unstable points after the minimisation of the existing system in two dimensions.

7. CONCLUSION

In conclusion, this study has conducted a comprehensive analysis of the Quasi-Geostrophic Omega Equation and the Lorenz-96 Model, shedding light on their attractor properties and dynamics. Through a combination of numerical simulations and analytical techniques, we have revealed the distinct behaviors exhibited by these systems. The stable and predictable nature of the QG Omega Equation contrasts sharply with the chaotic dynamics of the Lorenz-96 Model, underscoring the diverse range of behaviors present in atmospheric systems.

From the present work, we get a focused analysis on these two dynamical systems, including visualizations, formal proofs of the existence of global attractors, numerical methods to observe their behavior and stability, the transformation of the Lorenz-96 model in matrix form with methods from linear algebra, and the incorporation of stochastic parameters into the ODEs. This combination of formal proofs and programming tools allows us to describe dynamical systems with practical applications, such as meteorological models, as demonstrated here.

More specifically, in this article:

- We have analyzed thoroughly the behavior of the QG Omega Equation and the Lorenz-96 model, which are non-chaotic and chaotic, respectively.
- We formally attempted to prove the existence of a global attractor for the 1D Lorenz-96 model using analytic methods and a Lyapunov function.
- Then, we transformed and then generalized the Lorenz-96 model in three dimensions, expressing the whole system in matrices, with linear algebraic methods (as vectors, matrices, blocks).
- Then we transformed it again with changes in two parameters for a more statistical approach (with stochastic parameters such as Wiener processes and diffusion coefficients).
- Finally, we minimized the 3D transformation of the Lorenz-96 model into its 2D version and then transformed it again in a minimal form of a 2D system of ODEs.
- In each of those stages, we have visualized using MATLAB, the attractors, the vector fields and the final phase portrait.

Moving forward, the insights gained from this study have implications for weather forecasting and climate modeling efforts. By incorporating the findings into predictive models, we can improve the accuracy and reliability of weather forecasts and enhance our understanding of long-term climate trends. Overall, this study advances our knowledge of atmospheric dynamics and lays the groundwork for future research in the field.

ACKNOWLEDGMENT

We want to thank Dr. Dorotheos E. Aggelis for helping with the choice of the subject and supervising the progress of the manuscript. We would also like to thank the editor and the anonymous reviewers for their insightful comments and contributions.

Appendix - MATLAB scripts

Figure 1

```
f = 1;
g = 9.81;
```



```

Lx = 10;
Ly = 10;
nx = 20;
ny = 20;
x = linspace(0, Lx, nx);
y = linspace(0, Ly, ny);
[X, Y] = meshgrid(x, y);
u = -f * Y;
v = f * X;
figure;
quiver(X, Y, u, v);
xlabel('x');
ylabel('y');
title('Velocity Field for Quasi-Geostrophic Omega Equation (2D)');
axis equal;

```

```

f = 1;
g = 9.81;
Lx = 10;
Ly = 10;
Lz = 10;
nx = 20;
ny = 20;
nz = 20;
x = linspace(0, Lx, nx);
y = linspace(0, Ly, ny);
z = linspace(0, Lz, nz);
[X, Y, Z] = meshgrid(x, y, z);
u = -f * Y;
v = f * X;
w = g * ones(size(X));
figure;
quiver3(X, Y, Z, u, v, w);
xlabel('x');
ylabel('y');
zlabel('z');
title('Velocity Field for Quasi-Geostrophic Omega Equation (3D)');
axis equal;

```

Figure 2

```

f = 1;
f_qg = @(t, y) [-f * y(2); f * y(1); 0];
tspan = [0, 10];
num_trajectories = 10;
initial_conditions = 20 * rand(num_trajectories, 3);
trajectories = cell(num_trajectories, 1);
for i = 1:num_trajectories
    [-, y] = ode45(f_qg, tspan, initial_conditions(i, :));

```



```

trajectoriesi = y;
end
figure;
hold on;
for i = 1:num_trajectories
plot3(trajectoriesi(:, 1), trajectoriesi(:, 2), trajectoriesi(:, 3));
end
xlabel('x');
ylabel('y');
zlabel('z');
title('3D Attractor for Quasi-Geostrophic Omega Equation');
grid on;
hold off;

```

Figures 3, 4, 5

```

sigma = 10;
rho = 28;
beta = 8/3;
f_lorenz = @(t,y)[sigma * (y(2) - y(1)); y(1) * (rho - y(3)) - y(2); y(1) * y(2) - beta * y(3)];
tspan = [0, 50];
num_initial_conditions = 10;
initial_conditions = 40 * (rand(num_initial_conditions, 3) - 0.5);
trajectories = cell(num_initial_conditions, 1);
for i = 1:num_initial_conditions
[~, y] = ode45(f_lorenz, tspan, initial_conditions(i, :));
trajectoriesi = y;
end
figure;
hold on;
for i = 1:num_initial_conditions
plot3(trajectoriesi(:, 1), trajectoriesi(:, 2), trajectoriesi(:, 3));
end
xlabel('x');
ylabel('y');
zlabel('z');
title('3D Lorenz Attractor with Different Initial Conditions');
grid on;
hold off;

```

Figure 6

```

N = 40;
F = 8;
c = 10;
tspan = [0 50];
dt = 0.01;
x0_lorenz96 = randn(N, 1);
y0_lorenz96 = randn(N, 1);

```



```

z0_lorenz96 = randn(N, 1);
x0_omega = randn(N, 1);
y0_omega = randn(N, 1);
z0_omega = randn(N, 1);
odefun_lorenz96 = @(t, XYZ) lorenz96_3d(XYZ, N, F, c);
t_lorenz96, XYZ_lorenz96 = ode45(odefun_lorenz96, tspan, [x0_lorenz96; y0_lorenz96; z0_lorenz96]);
x_lorenz96 = XYZ_lorenz96(:, 1:N);
y_lorenz96 = XYZ_lorenz96(:, N+1:2*N);
z_lorenz96 = XYZ_lorenz96(:, 2*N+1:end);
figure;
plot3(x_lorenz96(:, y_lorenz96(:, z_lorenz96(:, 'b');
xlabel('x');
ylabel('y');
zlabel('z');
title('Attractor of the 3D Lorenz-96 Model');
grid on;
view(45, 30);
function dXYZdt = lorenz96_3d(XYZ, N, F, c)
x = XYZ(1:N);
y = XYZ(N+1:2*N);
z = XYZ(2*N+1:end);
dxdt = (circshift(y, -1) - circshift(z, 2)) .* circshift(x, -1) - x + F - (c / N) * (x - mean(x));
dydt = (circshift(z, -1) - circshift(x, 2)) .* circshift(y, -1) - y + F - (c / N) * (y - mean(y));
dzdt = (circshift(x, -1) - circshift(y, 2)) .* circshift(z, -1) - z + F - (c / N) * (z - mean(z));
dXYZdt = [dxdt; dydt; dzdt];
end

```

REFERENCES

- [1] T. Ak, A. Saha, S. Dhawan, and A. H. Kara, *Investigation of Coriolis effect on oceanic flows and its bifurcation via geophysical Korteweg–de Vries equation*, Numer. Methods Partial Differ. Equ., *36*(6) (2020), 1234-1253.
- [2] J. T. Allen, D. A. Smeed, A. J. G. Nurser, J. W. Zhang, and M. Rixen, *Diagnosis of vertical velocities with the QG omega equation: An examination of the errors due to sampling strategy*, Deep-Sea Res. I: Oceanogr. Res. Pap., *48*(2) (2001), 315-346.
- [3] A. Amemiya, M. Shlok, and T. Miyoshi, *Application of recurrent neural networks to model bias correction: Idealized experiments with the Lorenz-96 model*, J. Adv. Model. Earth Syst., *15*(2) (2023), e2022MS003164.
- [4] J. D. Annan and J. C. Hargreaves, *Efficient parameter estimation for a highly chaotic system*, Tellus A: Dyn. Meteorol. Oceanogr., *56*(5) (2004), 520-526.
- [5] H. Badawi, O. Abu Arqub, and N. Shawagfeh, *Stochastic integrodifferential models of fractional orders and Leffler nonsingular kernels: well-posedness theoretical results and Legendre Gauss spectral collocation approximations*, Chaos Solit. Fractals: X, *10* (2023), 100091.
- [6] D. Billingsley, *Review of QG theory—Part II: The omega equation*, Natl. Wea. Dig., *21*(2) (1997), 43-51.
- [7] J. Brajard, A. Carrassi, M. Bocquet, and L. Bertino, *Combining data assimilation and machine learning to emulate a dynamical model from sparse and noisy observations: A case study with the Lorenz 96 model*, J. Comput. Sci., *44* (2020), 101171.
- [8] D. S. Broomhead, R. Jones, G. P. King, and E. R. Pike, *Singular system analysis with application to dynamical systems*, In Chaos, noise and fractals, CRC Press, (2020), 15-27.
- [9] N. Črnjarić-Žic, S. Maćešić, and I. Mezić, *Koopman operator spectrum for random dynamical systems*, J. Nonlinear Sci., *30* (2020), 2007-2056.



- [10] G. S. Duane, *Synchronized chaos in extended systems and meteorological teleconnections*, PRE, 56(6) (1997), 6475.
- [11] D. J. Gagne, H. M. Christensen, A. C. Subramanian, and A. H. Monahan, *Machine learning for stochastic parameterization: Generative adversarial networks in the Lorenz'96 model*, J. Adv. Model. Earth Syst., 12(3) (2020), e2019MS001896.
- [12] N. Gkrekas, *Applying Laplace Transformation on Epidemiological Models as Caputo Derivatives*, Math. Biol. Bioinform., 19(1) (2024), 61-76.
- [13] W. He and J. Cao, *Generalized synchronization of chaotic systems: an auxiliary system approach via matrix measure*, Chaos, 19(1) (2009), 61-76.
- [14] J. R. Horton and G. J. Hakim, *An introduction to dynamic meteorology*, Academic Press, 88 (2013).
- [15] B. J. Hoskins, I. Draghici, and H. C. Davies, *A new look at the ω -equation*, Q. J. R. Meteorol. Soc., 104(439) (1978), 31-38.
- [16] B. Jiao, L. Ran, N. Li, R. Cai, T. Qu, and Y. Zhou, *Comparative Analysis of the Generalized Omega Equation and Generalized Vertical Motion Equation*, Adv. Atmos. Sci., 40(2023), 856-873.
- [17] A. Karimi and M. R. Paul, *Extensive chaos in the Lorenz-96 model*, Chaos, 20(4) (2010).
- [18] O. K. Koriko, K. S. Adegbe, A. S. Oke, and I. L. Animasaun, *Exploration of Coriolis force on motion of air over the upper horizontal surface of a paraboloid of revolution*, Phys. Scr., 95(3) (2020), 035210.
- [19] D. J. Lea, M. R. Allen, and T. W. Haine, *Sensitivity analysis of the climate of a chaotic system*, Tellus A: Dyn. Meteorol. Oceanogr., 52(5) (2000), 523-532.
- [20] E. N. Lorenz, *Deterministic nonperiodic flow*, JAS, 20(2) (1963), 130-141.
- [21] E. N. Lorenz and K. Haman, *The essence of chaos*, Pure Appl. Geophys., 147(3) (1996), 598-599.
- [22] B. Maayah, O. Abu Arqub, S. Alnabulsi, and H. Alsulami, *Numerical solutions and geometric attractors of a fractional model of the cancer-immune based on the Atangana-Baleanu-Caputo derivative and the reproducing kernel scheme*, Chin. J. Phys., 80 (2022), 463-483.
- [23] B. Maayah and O. Abu Arqub, *Adaptive the Dirichlet model of mobile/immobile advection/dispersion in a time-fractional sense with the reproducing kernel computational approach: Formulations and approximations*, Int. J. Mod. Phys. B, 37(18) (2023), 2350179.
- [24] B. Maayah, A. Moussaoui, S. Bushnaq, and O. Abu Arqub, *The multistep Laplace optimized decomposition method for solving fractional-order coronavirus disease model (COVID-19) via the Caputo fractional approach*, Demonstr. Math., 55(1) (2022), 963-977.
- [25] C. C. Maiocchi, V. Lucarini, A. Gritsun, and Y. Sato, *Heterogeneity of the attractor of the Lorenz'96 model: Lyapunov analysis, unstable periodic orbits, and shadowing properties*, Phys. D: Nonlinear Phenom., 457 (2024), 133970.
- [26] D. T. Mihailović, G. Mimić, and I. Arsenić, *Climate predictions: The chaos and complexity in climate models*, Adv. Meteorol., (2014).
- [27] H. Millán, A. Kalauzi, M. Cukic, and R. Biondi, *Nonlinear dynamics of meteorological variables: Multifractality and chaotic invariants in daily records from Pastaza, Ecuador*, Theor. Appl. Climatol., 102 (2002), 75-85.
- [28] C. Mou, Z. Wang, D. R. Wells, X. Xie, and T. Iliescu, *Reduced order models for the quasi-geostrophic equations: A brief survey*, Fluids, 6(1) (2020), 16.
- [29] I. Petromichelakis and I. A. Kougioumtzoglou, *Addressing the curse of dimensionality in stochastic dynamics: A Wiener path integral variational formulation with free boundaries*, Proc. R. Soc. A, 476(2243) (2020), 20200385.
- [30] B. Ramadevi and K. Bingi, *Chaotic Time Series Forecasting Approaches Using Machine Learning Techniques: A Review*, Symmetry, 10 (2022), 955.
- [31] I. Rizos and N. Gkrekas, *Can a mathematical model describe the main problems of the modern world?*, U.Porto J. Eng., 10(1) (2024), 59-68.
- [32] I. Rizos and N. Gkrekas, *Teaching and learning sciences within the COVID-19 pandemic era in a Greek university department*, U. Porto J. Eng., 8(1) (2022), 73-83.
- [33] J. L. Rodrigo, *On the evolution of sharp fronts for the quasi-geostrophic equation*, Commun. Pure Appl. Math., 58(6) (2005), 821-866.



- [34] A. M. Selvam, *Nonlinear dynamics and chaos: applications in meteorology and atmospheric physics*, Self-organized Criticality and Predictability in Atmospheric Flows: The Quantum World of Clouds and Rain, Springer, (2017), 1-40.
- [35] B. W. Shen, R. A. Pielke Sr., X. Zeng, J. J. Baik, S. Faghieh-Naini, J. Cui, R. Atlas, and T. A. L. Reyes, *Is Weather Chaotic? Coexisting Chaotic and Non-chaotic Attractors Within Lorenz Models*, In C. H. Skiadas, Y. Dimotikalis (eds) 13th Chaotic Modeling and Simulation International Conference, CHAOS 2020, Springer Proceedings in Complexity, (2020).
- [36] Q. Sun, T. Miyoshi, and S. Richard, *Control simulation experiments of extreme events with the Lorenz-96 model*, Nonlin. Processes Geophys., (2022), 1-18.
- [37] G. F. Weber, *Information Dynamics in Complex Systems Negates a Dichotomy between Chance and Necessity*, Information, 11 (2020), 245.
- [38] D. S. Wilks, *Effects of stochastic parametrizations in the Lorenz'96 system*, Q. J. R. Meteorol. Soc., 131(606) (2005), 389-407.
- [39] J. Wu, *The quasi-geostrophic equation and its two regularizations*, Commun. Partial Differ. Equ., 27(5-6) (2002), 1161-1181.
- [40] X. Yin, Q. Liu, S. Ma, and S. Bai, *Solitonic interactions for Rossby waves with the influence of Coriolis parameters*, Results Phys., 28 (2021), 104593.
- [41] Y. Zhang, Z. Hua, H. Bao, H. Huang, and Y. Zhou, *An n-dimensional chaotic system generation method using parametric Pascal matrix*, IEEE Trans. Ind. Inform., 18(12) (2022), 8434-8444.
- [42] R. Zhang and L. Yang, *Theoretical analysis of equatorial near-inertial solitary waves under complete Coriolis parameters*, AOS, 40 (2021), 54-61.
- [43] Y. Zheng and N. Li, *Non-asymptotic identification of linear dynamical systems using multiple trajectories*, IEEE Control Syst. Lett., 5(5) (2020), 1693-1698.

